Gas Storage

DOI: 10.1002/ange.201106615

A Highly Porous and Robust (3,3,4)-Connected Metal–Organic Framework Assembled with a 90° Bridging-Angle Embedded Octacarboxylate Ligand**

*Weigang Lu, Daqiang Yuan, Trevor A. Makal, Jian-Rong Li, and Hong-Cai Zhou**

Metal–organic frameworks (MOFs) are newly emerging porous materials that feature well-defined crystal structures.[1] Owing to their high specific surface areas, tunable structures and functionalities, they have been extensively studied for applications in the areas of gas storage and separation, particularly for hydrogen, methane, and carbon dioxide.[2]

In general, MOF structures may be viewed as having two main components: the organic linker and the inorganic metal cluster (also known as secondary building unit, SBU). It is well-established that the combination of both components governs the final framework topology, which in turn determines the performance as a storage or separation medium. The dinuclear paddle-wheel cluster, a square building unit, is one of the commonly used SBUs in the isoreticular synthesis of MOFs owing to its ability to form innumerous structures with a large range of organic ligands. We are particularly interested in the dicopper(II) paddle-wheel cluster because of its enhanced moisture resistance over the Zn_4O cluster[3] and genesis of exposed metal sites after the removal of axially coordinated solvent molecules. The presence of open metal sites in the framework facilitates H_2 storage owing to the strong metal–H_2 interaction.[4]

Ideally, the method to maximize surface area is to use long, slim organic linkers. However, elongation of organic ligands often yields fragile or interpenetrated frameworks, which generally have a negative impact on gas-uptake capacity.[5]

To design and construct non-interpenetrated MOFs, one powerful strategy is utilizing metal–organic polyhedra (MOPs) as supermolecular building blocks (SBBs).[6] Furthermore, a strategy employing dendritic ligands could possibly render MOFs with tolerance to slim organic linkers because of high connectivity. For example, the MOF assembled with 3-connected bte (for the definition see reference [7]) and dicopper(II) paddle-wheel cluster collapsed upon removal of guest solvents; however, a robust MOF (PCN-61, PCN stands for porous coordination network with permanent porosity)[8] was obtained when 6-connected btei[7] (having the same core structure as bte) was used instead. Moreover, by stepwise extension of the ligands from btei to the almost doubly-expanded ttei,[7] a family of highly porous and robust MOFs (PCN-6X) with cuboctahedral cages as the SBBs was obtained. It is noteworthy to mention that members of the PCN-6X family exhibit exceptionally high surface areas and gas-uptake capacities with no interpenetration observed, even in the ttei case.[9] This systematic study of the extension of dendritic ligands emphasized the positive correlation between ligand connectivity and framework stability.

Inspired by the successes of PCN-6X, we continued to explore SBBs other than cuboctahedral cages[10] as well as more dendritic ligands in the search for MOFs with ultrahigh surface area without compromising stability.

So far, cuboctahedral cages have been the most frequently used SBBs owing to the chemical accessibility of 120°-angular-dicarboxylate ligands. However, octahedral cages, other geometrically versatile building blocks that can be assembled with 90°-angular-dicarboxylate ligands and dicopper(II) paddle-wheel cluster,[11] have rarely been studied in the construction of three-dimensional MOFs, which is likely due to the difficulty in the ligand synthesis.

Herein we report the design and synthesis of a highly porous and robust dicopper(II)-paddle-wheel-based metal–organic framework (PCN-80). To our knowledge, PCN-80 is a rare example of MOF assembled with an octatopic ligand[12] and the first one that features a 90°-bridging-angle subunit.

The octatopic ligand 9,9′,9″,9‴-([1,1′-biphenyl]-3,3′,5,5′-tetrayl)tetrakis(9H-carbazole-3,6-dicarboxylic acid) (H_8bttcd) was synthesized by a Cu^I-catalyzed reaction between dimethyl 9H-carbazole-3,6-dicarboxylate and 3,3′,5,5′-tetrabromo-1,1′-biphenyl and subsequent hydrolysis with KOH in an overall yield of 30% (Scheme 1). This unique ligand has a 90°-angular-dicarboxylate moiety as opposed to the widely used 120°-angular-isophthalate moiety in the construction of MOFs (Scheme 1).

Solvothermal reaction of H_8bttcd and $Cu(NO_3)_2{\cdot}2.5H_2O$ in DMF (*N*,*N*-dimethylformamide) in the presence of HBF_4 afforded tetragonal-shaped green crystals of PCN-80 with the molecular formula $[Cu_2(bttcd)]{\cdot}2$ DMF. PCN-80 crystallizes in

[*] Dr. W. Lu, Dr. D. Yuan, T. A. Makal, Dr. J.-R. Li, Prof. Dr. H.-C. Zhou
Department of Chemistry, Texas A&M University
College Station, TX 77842 (USA)
E-mail: zhou@mail.chem.tamu.edu
Homepage: http://www.chem.tamu.edu/rgroup/zhou/

[**] This work was supported by the U.S. Department of Energy (DOE DE-SC0001015, DE-FC36-07GO17033, and DE-AR0000073), the National Science Foundation (NSF CBET-0930079 and CHE-0911207), and the Welch Foundation (A-1725) supported this work. The microcrystal diffraction of PCN-80 was carried out with the assistance of Yu-Sheng Chen at the Advanced Photon Source on beamline 15ID-B at ChemMatCARS Sector 15, which is principally supported by the NSF/DOE under grant number CHE-0535644. Use of the Advanced Photon Source was supported by the U. S. DOE, Office of Science, Office of Basic Energy Sciences, under Contract No. DE-AC02-06CH11357.

Supporting information for this article is available on the WWW under http://dx.doi.org/10.1002/anie.201106615.

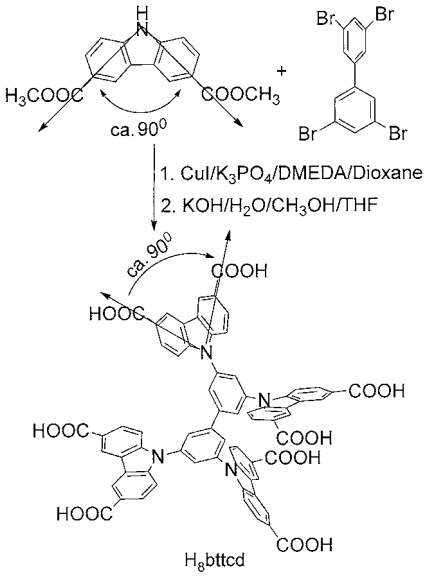

Scheme 1. Synthesis of H_8bttcd. DMEDA = *N*,*N*′-dimethylethylenediamine.

tetragonal *I*4/*mmm* space group with $a = b = 23.057(2)$, $c = 30.762(3)$ Å. In the structure of PCN-80, the bttcd ligand contains four 90°-angle subunits (Figure 1a) where the carbazole ring is perpendicular to the central benzene ring and the dihedral angle between adjacent carbazole rings is 47.4°. Every bttcd ligand utilizes eight carboxylate groups to link eight 4-connected dicopper paddle-wheel SBUs (Figure 1b) in a rectangular prismatic fashion to generate a porous (3,3,4)-connected network. There are three kinds of microporous cages with different sizes. L-cages (16.6 Å in diameter) are formed by eight $[Cu_2(O_2CR)_4]$ SBUs and twelve bttcd linkers (Figure 1c), M-cages (13.4 Å) from eight SBUs and four bttcd linkers (Figure 1d), and S-cages (7.6 Å) through four SBUs and two bttcd ligands (Figure 1e). The overall structure consists of these three types of cages packed in a 1:1:1 ratio (Figure 1f). From the viewpoints of topology, the SBUs serve as 4-connected nodes, whereas bttcd ligands as 3,3-connected nodes. As a result, PCN-80 adopts the very rare 3,3,4-c 3-nodal net (Figure 1g) with topological point symbol of $\{7^2.8^2.11^2\}\{7^2.8\}\{7^3\}_2$, which is previously unreported. If the bttcd ligand is further simplified as 8-connected node, PCN-80 has a 4,8-c 2-nodal net with scu topology (Figure S18 in the Supporting Information), which is rarely reported in MOFs.[12a,b,13]

The calculated free volume in fully desolvated PCN-80 is 72.1% by PLATON (1.8 Å probe radius), and the pore volume is 1.25 $cm^3 g^{-1}$. To confirm the porosity, PCN-80 was degassed under dynamic vacuum at 80 °C for ten hours after solvent exchange with methanol and then dichloromethane. A color change from green to deep purple-blue was observed, typical for dicopper(II)-paddle-wheel frameworks in which open copper sites are generated. The N_2 sorption for PCN-80 at 77 K exhibited a reversible type-I isotherm, a characteristic of microporous materials. The estimated apparent BET surface area was approximately 3850 $m^2 g^{-1}$ (calculated ca. 3584 $m^2 g^{-1}$) and Langmuir surface area approximately

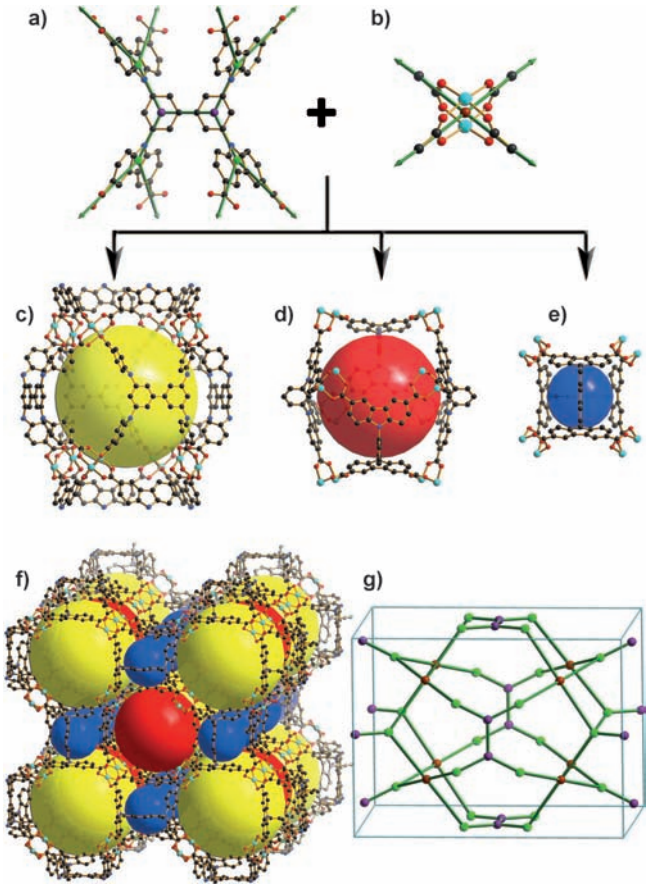

Figure 1. a) 8-connected bttcd ligand; b) 4-connected dicopper(II) paddle-wheel SBU; c) large-size cage (L-cage); d) middle-size cage (M-cage); e) small-size cage (S-cage); f) cages and their 3D packing in PCN-80; g) topology of PCN-80.

4150 $m^2 g^{-1}$, which is similar to PCN-66 (BET ca. 4000 $m^2 g^{-1}$), among the highest reported to date for porous MOFs or covalent organic frameworks (COFs). Notably, the experimental surface area of PCN-80 perfectly agrees with that calculated using Materials Studio 5.5. On the basis of the N_2 sorption isotherm, PCN-80 has a calculated total pore volume of 1.47 $cm^3 g^{-1}$. Calculated with N_2 isotherm using DFT methods, the pore size distribution for PCN-80 (inset of Figure 2a) indicates three different kinds of pores with diameters of 7.3, 11.8, and 14.5 Å, respectively, which is in good agreement with the crystal data (Figure 2b).

It is well-known that in the low-pressure region the H_2-uptake capacity is mainly controlled by the hydrogen affinity towards the framework. PCN-80 exhibits H_2-uptake capacity as high as 2.3 wt% at 77 K and 1 bar (Figure 3a), which is among the highest at low pressure.[4b,12a,14] The excellent performance of PCN-80 can be largely attributed to its microporous nature as well as high open-metal-site density upon activation.

High-pressure gas sorption was performed on PCN-80 using volumetric measurement method. At 77 K, the excess H_2-uptake capacity of PCN-80 reached its maximum value of 4.8 wt% (29 $g L^{-1}$) at 44 bar. The values are comparable to MOFs with similar surface areas, such as IRMOF-20[15] (S_{BET}:

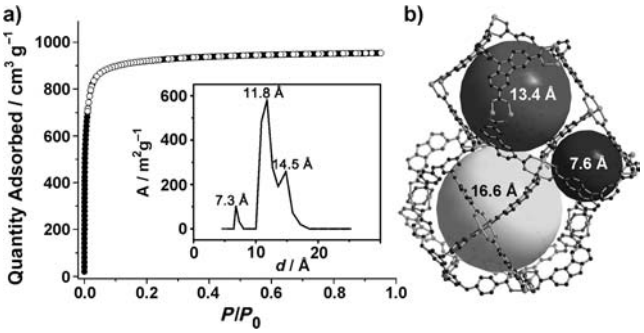

Figure 2. a) Experimental N_2 sorption isotherm for PCN-80 at 77 K; ● adsorption, ○ desorption. Inset shows the pore size distribution (incremental surface area (*A*) vs. pore width (*d*)); b) ball packing in PCN-80 showing three different sized cages.

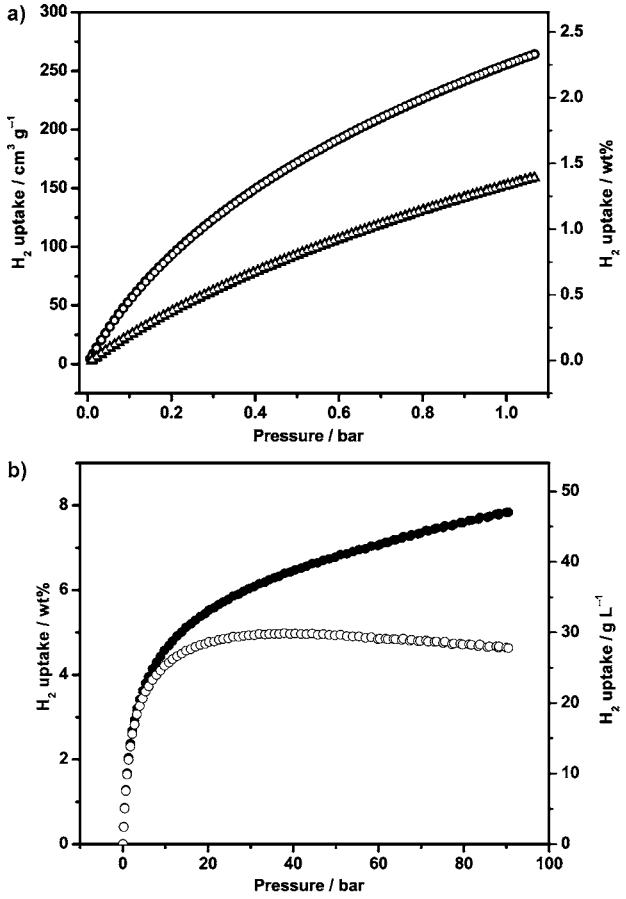

Figure 3. H_2 uptake for PCN-80 a) at low pressure (at 77 K: ● adsorption, ○ desorption; at 87 K: ▲ adsorption, △ desorption) and b) at high pressure (77 K; ● total uptake, ○ excess uptake).

4024 $m^2 g^{-1}$, 6.25 excess/wt%, 34.1 vol./g L^{-1} at 77.6 bar), Be(BTB)[16] (S_{BET}: 4030 $m^2 g^{-1}$, 6.0 excess/wt%, 28.1 vol./g L^{-1} at 20 bar), PCN-66[9a] (S_{BET}: 4000 $m^2 g^{-1}$, 6.2 excess/wt%, 29.6 vol./g L^{-1} at 45 bar), MIL-101[17] ($S_{Langmuir}$: 5500 $m^2 g^{-1}$, 6.1 excess/wt%, 26.1 vol./g L^{-1} at 80 bar). Taking into consideration the gaseous hydrogen compressed within the framework void, its total H_2 uptake was 7.7 wt% (48 g L^{-1}) at 90 bar (Figure 3b). At 296 K, the excess CH_4-uptake capacity of PCN-80 is 147 mg g^{-1} (118 $cm^3 cm^{-3}$ based on the crystallographic density) at 35 bar (Figure S5 in the Supporting Information); the excess CO_2-uptake capacity can reach 670 mg g^{-1} (195 $cm^3 cm^{-3}$) at 20 bar (Figure S6 in the Supporting Information). The robustness of PCN-80 was corroborated by comparing powder X-ray diffraction (PXRD) pattern of the sample after high-pressure-uptake measurements with the simulated pattern generated from single-crystal XRD data (Figure 4). To further understand the effect of moisture on PCN-80, activated PCN-80 was exposed to air

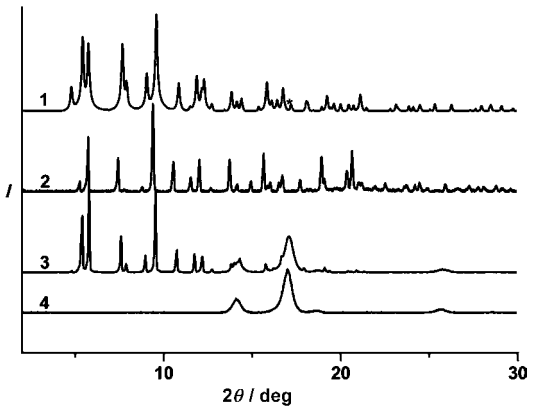

Figure 4. PXRD patterns of PCN-80: 1) simulated from the crystallographic information file (CIF), 2) from the as-synthesized PCN-80, 3) from the desolvated PCN-80, 4) background of desolvated PCN-80.

and analyzed by PXRD (Figure S17 in the Supporting Information). The stability of PCN-80 seems lower than that of HKUST-1,[3] bearing the same dicopper(II) paddle-wheel cluster, possibly owing to the larger pores in PCN-80.

Carbon capture and sequestration (CCS) has been proposed as a feasible method for controlling atmospheric carbon dioxide concentration. Currently, the capture processes in large-scale operation utilize amine-based wet scrubbing systems, which require high energy and resource consumption.[18] MOF-based porous materials have been proven to be good absorbents for CO_2 at ambient temperature and the physisorption mechanism makes their recycling less energy-intensive. This prompted us to measure CO_2 and N_2 sorption for PCN-80 at ambient temperature. As shown in Figure 5, PCN-80 exhibits remarkable CO_2-uptake capacity (19.3 and 12.0 wt% at 273 and 296 K, respectively) and very little N_2-uptake capacity (0.73 and 0.34 wt% at 273 and 296 K, respectively). Although the CO_2-uptake capacity of PCN-80 is considerably below the highest recorded to date (Mg/DOBDC,[19] 35.2 wt% at 296 K), it is among the highest for a metal–organic framework based on dicopper(II) paddle-wheel clusters.[2i] By determining the Henry's law constants with single gas adsorption isotherms,[20] the CO_2/N_2 adsorption selectivity factors for PCN-80 are 18.7 and 11.8 at 273 and 296 K, respectively.

In summary, a highly porous and robust MOF (PCN-80) with a rare (3,3,4)-connected network topology has been

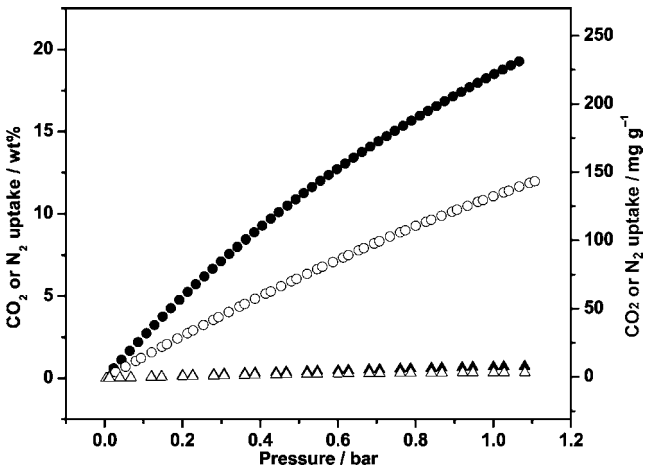

Figure 5. Gravimetric CO_2 and N_2 adsorption isotherms for PCN-80 at 273 K (● CO_2, ▲ N_2) and 296 K (○ CO_2, △ N_2).

synthesized by using a unique octatopic ligand featuring 90°-angle-dicarboxylate moieties. PCN-80 exhibits high gas-uptake capacity in H_2 and large adsorption selectivity of CO_2 over N_2. Interestingly, the octahedral cage, thermodynamically assembled from carbazole-3,6-dicarboxylate ligand and dicopper(II) paddle-wheel cluster,[11a] did not form in this structure as we expected, nonetheless, this work will not only enrich the diversity of MOF topologies, but also be beneficial for the understanding of the correlation between high connectivity and framework stability. We surmise robust MOFs with much higher surface area can be achieved by extending the dendritic ligand. Work along this line is currently underway.

Experimental Section

H_8bttcd: Dimethyl 9*H*-carbazole-3,6-dicarboxylate (1.8 g, 6.4 mmol), K_3PO_4 (3.0 g, 14.2 mmol), 3,3′,5,5′-tetrabromo-1,1′-biphenyl (0.7 g, 1.5 mmol), CuI (60 mg, 0.32 mmol), DMEDA (*N*,*N*′-dimethylethylenediamine, 0.1 mL), dioxane (20 mL), and a stir bar were added to a sealable flask in nitrogen. The resulting mixture was sealed and heated to 120 °C for three days. After cooling to room temperature, water was added, the precipitate collected, washed with ethyl acetate and acetone, then suspended in a mixture of THF/MeOH (100 mL, v/v = 1:1) and 50 mL KOH (2 mol L^{-1}). The resultant was stirred and heated to reflux until a clear solution was obtained. After the solution was cooled to room temperature, organic solvents were removed, and then the aqueous solution was acidified with HCl (1N). The precipitate was collected and washed with water. Recrystallization with DMSO/MeOH produced 0.6 g of H_8bttcd. Elemental analysis (%): calcd for $C_{68}H_{38}N_4O_{16}$: C 69.98, H 3.28, N 4.80, O 21.93; found: C 69.83, H 3.40, N 4.78. ^{1}H NMR (300 MHz, [D_6]DMSO): $\delta = 7.72$ (8H, d, $J = 9.0$ Hz), 8.11 (10H, m), 8.65 (4H, d, $J = 0.9$ Hz), 8.95 (8H, d, $J = 1.5$ Hz), 12.78 ppm (4H, br).

PCN-80: A mixture of H_8bttcd (10 mg, 0.0086 mmol) and $Cu(NO_3)_2{\cdot}2.5H_2O$ (15 mg, 0.016 mmol) was added to a small vial containing DMF (2 mL), and 1 drop of HBF_4. The vial was sealed, heated to 75 °C overnight, and the green block crystals of PCN-80 were collected, washed with DMF, and dried in air. Yield: 8.0 mg, 65% based on H_8bttcd. Elemental analysis calcd (%) for $C_{34}H_{19}Cu_2N_2O_{10}$: C, 54.99; H, 2.58; Cu, 17.11; N, 3.77; O, 21.54; found: C 37.47, H 5.15, N 8.30.

Crystal data for PCN-80: $C_{34}H_{19}Cu_2N_2O_{10}$, $M = 742.59$, green block, $0.12 \times 0.08 \times 0.07$ mm^3, tetragonal, space group *I*4/*mmm* (No. 139), $a = b = 23.057(2)$, $c = 30.762(3)$ Å, $V = 16354(3)$ Å^3, $Z = 16$, $\rho_{cald} = 0.643$ g cm^{-3}, $F_{000} = 3120$, synchrotron radiation, $\lambda = 0.40663$ Å, $T = 173(2)$ K, $2\theta_{max} = 22.4°$, 60183 reflections collected, 2121 unique ($R_{int} = 0.2501$). Final $GooF = 1.234$, $R1 = 0.1276$, $wR2 = 0.3368$, R indices based on 1160 reflections with $I > 2\sigma(I)$ (refinement on F^2), 120 parameters, 72 restraints. Lp and absorption corrections applied, $\mu = 0.122$ mm^{-1}. CCDC 804639 contains the supplementary crystallographic data for this paper. These data can be obtained free of charge from The Cambridge Crystallographic Data Centre via www.ccdc.cam.ac.uk/data_request/cif.

Full experimental details, thermogravimetric analysis, IR and NMR spectroscopy, and extra gas sorption isotherms are presented in the Supporting Information.

Received: September 18, 2011
Revised: November 23, 2011
Published online: January 13, 2012

Keywords: carbon dioxide fixation · hydrogen storage · metal–organic frameworks · carboxylate ligands

[1] a) O. M. Yaghi, M. O'Keeffe, N. W. Ockwig, H. K. Chae, M. Eddaoudi, J. Kim, *Nature* **2003**, *423*, 705 – 714; b) S. Kitagawa, R. Kitaura, S.-i. Noro, *Angew. Chem.* **2004**, *116*, 2388 – 2430; *Angew. Chem. Int. Ed.* **2004**, *43*, 2334 – 2375; c) G. Férey, *Chem. Soc. Rev.* **2008**, *37*, 191 – 214; d) D. Zhao, D. J. Timmons, D. Yuan, H.-C. Zhou, *Acc. Chem. Res.* **2010**, *44*, 123 – 133; e) J. R. Long, O. M. Yaghi, *Chem. Soc. Rev.* **2009**, *38*, 1213 – 1214.

[2] a) D. Zhao, D. Yuan, H.-C. Zhou, *Energy Environ. Sci.* **2008**, *1*, 222 – 235; b) J. Sculley, D. Yuan, H.-C. Zhou, *Energy Environ. Sci.* **2011**, *4*, 2721 – 2735; c) L. J. Murray, M. Dinca, J. R. Long, *Chem. Soc. Rev.* **2009**, *38*, 1294 – 1314; d) M. Hirscher, *Angew. Chem.* **2011**, *123*, 605 – 606; *Angew. Chem. Int. Ed.* **2011**, *50*, 581 – 582; e) S. Ma, H.-C. Zhou, *Chem. Commun.* **2010**, *46*, 44 – 53; f) W. Zhou, *Chem. Rec.* **2010**, *10*, 200 – 204; g) D. M. D'Alessandro, B. Smit, J. R. Long, *Angew. Chem.* **2010**, *122*, 6194 – 6219; *Angew. Chem. Int. Ed.* **2010**, *49*, 6058 – 6082; h) J.-R. Li, R. J. Kuppler, H.-C. Zhou, *Chem. Soc. Rev.* **2009**, *38*, 1477 – 1504; i) J.-R. Li, Y. Ma, M. C. McCarthy, J. Sculley, J. Yu, H.-K. Jeong, P. B. Balbuena, H.-C. Zhou, *Coord. Chem. Rev.* **2011**, *255*, 1791 – 1823.

[3] K. A. Cychosz, A. J. Matzger, *Langmuir* **2010**, *26*, 17198 – 17202.

[4] a) D. J. Collins, H.-C. Zhou, *J. Mater. Chem.* **2007**, *17*, 3154 – 3160; b) M. Dincă, J. R. Long, *Angew. Chem.* **2008**, *120*, 6870 – 6884; *Angew. Chem. Int. Ed.* **2008**, *47*, 6766 – 6779; c) J. L. C. Rowsell, O. M. Yaghi, *Angew. Chem.* **2005**, *117*, 4748 – 4758; *Angew. Chem. Int. Ed.* **2005**, *44*, 4670 – 4679; d) J. G. Vitillo, L. Regli, S. Chavan, G. Ricchiardi, G. Spoto, P. D. C. Dietzel, S. Bordiga, A. Zecchina, *J. Am. Chem. Soc.* **2008**, *130*, 8386 – 8396; e) K. Gedrich, I. Senkovska, N. Klein, U. Stoeck, A. Henschel, M. R. Lohe, I. A. Baburin, U. Mueller, S. Kaskel, *Angew. Chem.* **2010**, *122*, 8667 – 8670; *Angew. Chem. Int. Ed.* **2010**, *49*, 8489 – 8492.

[5] a) J. K. Schnobrich, K. Koh, K. N. Sura, A. J. Matzger, *Langmuir* **2010**, *26*, 5808 – 5814; b) X. Lin, J. Jia, P. Hubberstey, M. Schroder, N. R. Champness, *CrystEngComm* **2007**, *9*, 438 – 448; c) B. Chen, M. Eddaoudi, S. T. Hyde, M. O'Keeffe, O. M. Yaghi, *Science* **2001**, *291*, 1021 – 1023.

[6] a) A. J. Cairns, J. A. Perman, L. Wojtas, V. C. Kravtsov, M. H. Alkordi, M. Eddaoudi, M. J. Zaworotko, *J. Am. Chem. Soc.* **2008**, *130*, 1560 – 1561; b) F. Nouar, J. F. Eubank, T. Bousquet, L. Wojtas, M. J. Zaworotko, M. Eddaoudi, *J. Am. Chem. Soc.* **2008**, *130*, 1833 – 1835; c) S.-T. Zheng, T. Wu, B. Irfanoglu, F. Zuo, P.

Feng, X. Bu, *Angew. Chem.* **2011**, *123*, 8184 – 8187; *Angew. Chem. Int. Ed.* **2011**, *50*, 8034 – 8037.
[7] bte: 4,4′,4″-[benzene-1,3,5-triyl-tris(ethyne-2,1-diyl)]tribenzoate; btei: 5,5′,5″-[benzene-1,3,5-triyl-tris(ethyne-2,1-diyl)]triisophthalate; ttei: 5,5′,5″-({[benzene-1,3,5-triyl-tris(ethyne-2,1-diyl)]tris(benzene-4,1-diyl)}tris(ethyne-2,1-diyl))triisophthalate.
[8] D. Zhao, D. Yuan, D. Sun, H.-C. Zhou, *J. Am. Chem. Soc.* **2009**, *131*, 9186 – 9188.
[9] a) D. Yuan, D. Zhao, D. Sun, H.-C. Zhou, *Angew. Chem.* **2010**, *122*, 5485 – 5489; *Angew. Chem. Int. Ed.* **2010**, *49*, 5357 – 5361; b) O. K. Farha, A. Özgür Yazaydın, I. Eryazici, C. D. Malliakas, B. G. Hauser, M. G. Kanatzidis, S. T. Nguyen, R. Q. Snurr, J. T. Hupp, *Nat. Chem.* **2010**, *2*, 944 – 948.
[10] a) J.-R. Li, H.-C. Zhou, *Nat. Chem.* **2010**, *2*, 893 – 898; b) J.-R. Li, H.-C. Zhou, *Angew. Chem.* **2009**, *121*, 8617 – 8620; *Angew. Chem. Int. Ed.* **2009**, *48*, 8465 – 8468.
[11] a) J.-R. Li, D. J. Timmons, H.-C. Zhou, *J. Am. Chem. Soc.* **2009**, *131*, 6368 – 6369; b) Z. Ni, A. Yassar, T. Antoun, O. M. Yaghi, *J. Am. Chem. Soc.* **2005**, *127*, 12752 – 12753.
[12] a) L. Ma, D. J. Mihalcik, W. Lin, *J. Am. Chem. Soc.* **2009**, *131*, 4610 – 4612; b) C. Tan, S. Yang, N. R. Champness, X. Lin, A. J. Blake, W. Lewis, M. Schroder, *Chem. Commun.* **2011**, *47*, 4487 – 4489; c) Z.-J. Lin, T.-F. Liu, B. Xu, L.-W. Han, Y.-B. Huang, R. Cao, *CrystEngComm* **2011**, *13*, 3321 – 3324.
[13] X. Duan, X. Cheng, J. Lin, S. Zang, Y. Li, C. Zhu, Q. Meng, *CrystEngComm* **2008**, *10*, 706 – 714.
[14] a) O. K. Farha, A. M. Spokoyny, K. L. Mulfort, M. F. Hawthorne, C. A. Mirkin, J. T. Hupp, *J. Am. Chem. Soc.* **2007**, *129*, 12680 – 12681; b) S. Hong, M. Oh, M. Park, J. W. Yoon, J.-S. Chang, M. S. Lah, *Chem. Commun.* **2009**, 5397 – 5399; c) X.-S. Wang, S. Ma, P. M. Forster, D. Yuan, J. Eckert, J. J. López, B. J. Murphy, J. B. Parise, H.-C. Zhou, *Angew. Chem.* **2008**, *120*, 7373 – 7376; *Angew. Chem. Int. Ed.* **2008**, *47*, 7263 – 7266.
[15] A. G. Wong-Foy, A. J. Matzger, O. M. Yaghi, *J. Am. Chem. Soc.* **2006**, *128*, 3494 – 3495.
[16] K. Sumida, M. R. Hill, S. Horike, A. Dailly, J. R. Long, *J. Am. Chem. Soc.* **2009**, *131*, 15120 – 15121.
[17] M. Latroche, S. Surblé, C. Serre, C. Mellot-Draznieks, P. L. Llewellyn, J.-H. Lee, J.-S. Chang, S. H. Jhung, G. Férey, *Angew. Chem.* **2006**, *118*, 8407 – 8411; *Angew. Chem. Int. Ed.* **2006**, *45*, 8227 – 8231.
[18] J. D. Figueroa, T. Fout, S. Plasynski, H. McIlvried, R. D. Srivastava, *Int. J. Greenhouse Gas Control* **2008**, *2*, 9 – 20.
[19] S. R. Caskey, A. G. Wong-Foy, A. J. Matzger, *J. Am. Chem. Soc.* **2008**, *130*, 10870 – 10871.
[20] M. S. Sun, D. B. Shah, H. H. Xu, O. Talu, *J. Phys. Chem. B* **1998**, *102*, 1466 – 1473.

